Journal of Structural Geology, Vol. 11, No. 4, pp. 463 to 472, 1989
Printed in Great Britain

0191-8141/89 $03.00 + 0.00

Deformed soft sediments at the junction between the Mariana and Yap Trenches

GAKU KIMURA

Department of Earth Sciences, Faculty of Education, Kagawa University, Takamatsu 760, Japan

KAZUHIDE KOGA

Ocean Research Institute, University of Tokyo, Minamidai, Nakanoku, Tokyo 164, Japan

and

KANTARO FUJIOKA

Ocean Research Institute, University of Tokyo, Minamidai, Nakanoku, Tokyo 164, Japan

(*Received* 12 *May* 1987; *accepted in revised form* 19 *October* 1988)

Abstract—Highly deformed unconsolidated hemipelagic sediments were found below the sea bed surface at anomalously shallow depths near the junction between the Mariana and Yap arc–trench systems. The order of deformation is (1) sigmoidal veins and spaced foliations, (2) layer-parallel shear planes, (3) reverse faults and kink bands and (4) more veins. All the deformation structures are considered to have been developed progressively during shear parallel to bedding, accompanied by volume decrease due to pore reduction and fluid expulsion during consolidation, while the sediments are not yet lithified.

INTRODUCTION

DURING the cruise of R/V Hakuho-maru, KH86–1, Ocean Research Institute, University of Tokyo, highly deformed soft hemipelagic sediments were found in piston core samples taken from the shallow part of the sediment pile at the lowest part of the inner trench slope at the junction between the Mariana and Yap Trenches, along the southeastern margin of the Philippine Sea plate. The small-scale deformation features in the core were quite different from other Deep Sea Drilling Project (DSDP) cores. In the case of the DSDP cores, structures characteristic of layer-parallel compression or shear typically dominate at sites on the lower slope (e.g. off Mexico, Nankai, Barbados), whereas those indicative of layer-parallel extension are mainly formed at sites on the upper slope (Lundberg & Moore 1986). The former deformation is ascribed directly to subduction and the latter to downslope movement of the upper layers of sediments along low-angle detachment surfaces on the slope (Knipe 1986, Lundberg & Moore 1986). The piston core in this study, however, represents both types of deformation structures; both extension and compression must have been developed at shallow depths beneath the sea bed. The *in situ* orientation of the rotated core has been reconstructed on the basis of paleomagnetic analysis. The veins and other structures appear to have been formed as a result of shear parallel to the layering, possibly associated with the subduction of the Pacific plate or gravity sliding related to tectonism. In this paper, we describe the nature of the deformation structures and discuss the mechanisms of their formation.

TECTONIC SETTING

The piston core sample, P-1, was recovered from the area where the Mariana and Yap arc–trench systems meet and the Caroline Ridge on the Pacific plate collides with them (Figs. 1a & b). The Pacific plate is moving toward the WNW at about 11 cm yr^{-1} (Minster & Jordan 1978) and is being subducted beneath the southeastern margin of the Philippine Sea plate.

As shown in Fig. 1(b), the Mariana Trench floor is rimmed by three slopes at its western end; the southward-dipping landward slope of the Mariana Trench, the northwestern slope of the Caroline Ridge and the northeastern slope of an unnamed swell observed between the Caroline Ridge and Yap Trench. Five bench-like structures are recognizable on precise depth records at the foot of the northeastern slope of the unnamed swell; site P-1 is located on the fourth bench above the trench floor (Fig. 1c).

DESCRIPTION OF DEFORMED SEDIMENTS

Procedure

The core sample P-1, 3.775 m long, was cut into three sections and each split into two halves. We examined the

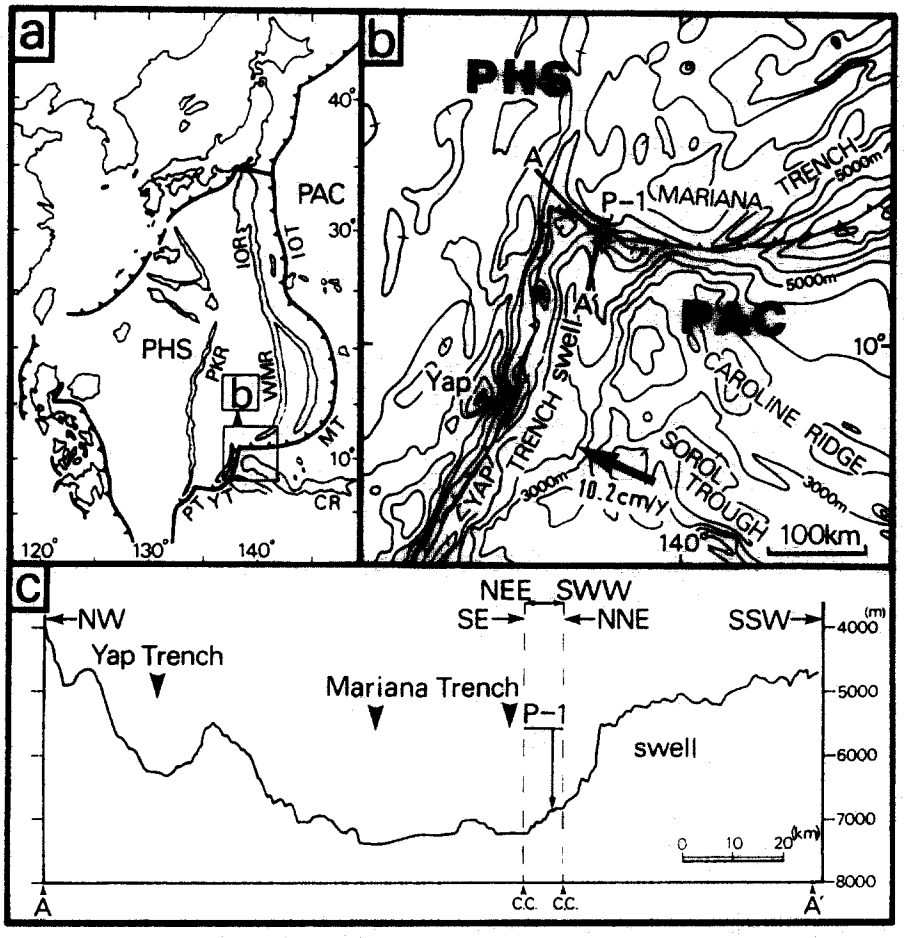

Fig. 1. Index map and profiles of sampling site, P-1, at the junction area between the Mariana and Yap trenches. (a) Arc–trench systems around the location of site P-1. Square area shows location of (b). IOT, Izu-Ogasawara Trench; MT, Mariana Trench; YT, Yap Trench; PT, Palau Trench; IOR, Izu-Ogasawara Ridge; CR, Caroline Ridge; PAC, Pacific plate; PHS, Philippine Sea plate. (b) Bathymetric and tectonic map showing the site P-1 and line A–A′ of precise depth record; contour interval is 1000 m. PAC, Pacific plate; PHS, Philippine Sea plate. (c) Profile based on precise depth record during the KH86-1 cruise; site P-1 is located on the fourth bench above the trench floor.

cut surface of the core carefully in order to find sedimentary and tectonic structures. Although the post-sedimentary and tectonic structures are invisible to the naked eye, they are easily recognizable using soft X-ray radiographs. These represent only two-dimensional traces of the structures; three-dimensional ones were partly obtained by radiographs taken from sub-slices perpendicular to the first surfaces, as well as horizontal sections of computed tomography scan (CT scan).

In order to determine the original orientation of the cores, the direction and intensity of their natural remnant magnetization (NRM) was measured using a spinner magnetometer. The top of the core sediment was magnetized parallel to the direction of the present geomagnetic field. Stability of NRM was assessed during alternating field demagnetization (AF). The orientations of the structures were determined after reorienting each core section. Azimuths of the two-dimensional vertical sketches from radiographs obtained in this way are shown in column D of Fig. 2. Occasional radiolarian fossils were found at some core intervals, although other microfossils were almost absent throughout the core. The radiolaria indicate Pliocene to Recent ages with some early to Middle Miocene reworked fossils (Okamura & Matsugi oral communication).

Paleomagnetic and geomagnetic reversal age determinations were carried out based on comparison of polarity changes throughout the core with established magnetic chronology (columns B and C in Fig. 2). The polarities were checked using the intensities and inclina-

Fig. 2. Core description and magnetic results. A–lithology, B–magnetic inclination, C–magnetic declination, D–sketches of deformation structures from soft X-ray radiographs, E–sketches from computed tomography scan. In B and C, solid and open symbols show normal and reverse magnetization, respectively. Square and triangles indicate the results of 25 œ and 50 œ demagnetization in the lower part of Section 3. In the other parts, the orientations are stable during progressive demagnetization. The azimuth of the soft X-ray radiograph of core Section 1 is N37.5°E, and its surface is observed from the NW. In Section 2, the azimuth of the radiograph is N61.3°W, and its surface is seen from the SW. In the Section 3, the azimuth of the radiograph is N84.4°E, and its surface is observed from the south. Sub-slice of Section 3 is observed from the east. The horizontal images of CT-scans are observed from above.

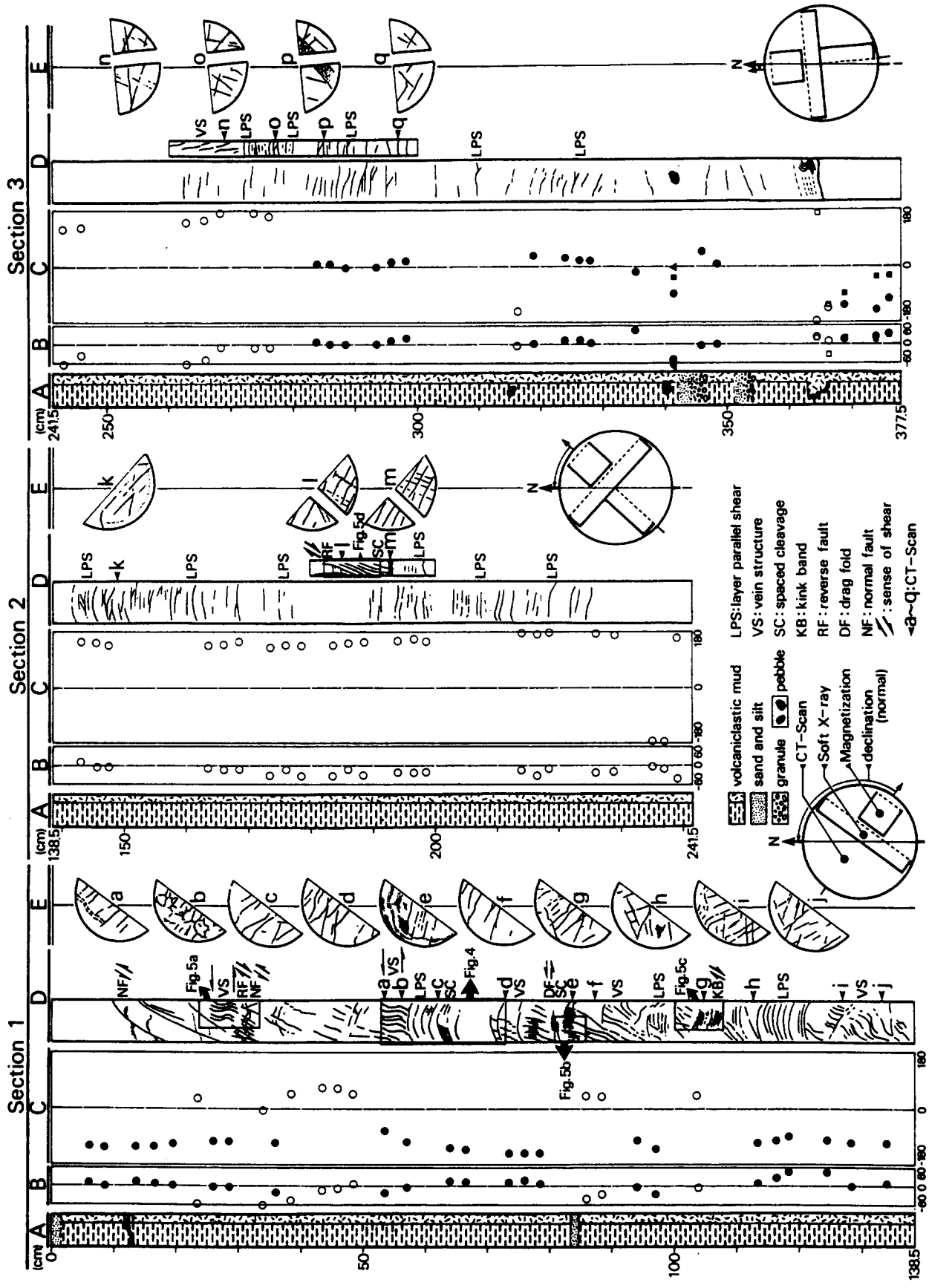
Section 1
Section 2
Section 3
LPS:layer parallel shear
VS:vein structure
SC:spaced cleavage
KB:kink band
RF:reverse fault
DF:drag fold
NF:normal fault
: sense of shear
a~Q:CT-Scan
volcaniclastic mud
sand and silt
granule
pebble
CT-Scan
Soft X-ray
Magnetization
declination
(normal)

Fig. 2.

tions of the sediment samples during progressive AF demagnetization. The uppermost part of the core has normal polarity, with stable NRM during progressive demagnetization. The first geomagnetic reversal was observed at 23.5 cm from the top of the core. It is likely that there may have been erosion or non-deposition at the top of the core, since the first reversal occurs at a depth shallower than that estimated from the Pliocene to Quaternary sedimentation rates (about 5 mm per 1000 yr) from the Mariana Trench margin and the Caroline Ridge (Burkry *et al.* 1971).

Sedimentary facies

The sediments are hemipelagic, composed mainly of moderately brown (5YR5/4) to moderately yellowish brown (10YR5/4) volcanoclastic mud with altered volcanic glass shards, feldspars, pyroxenes and hornblendes. They are not lithified and are easy to cut with a 'cheese-slicer'. Thin layers of volcanoclastic sand and silt are intercalated in Section 1 and consist mainly of the above mentioned minerals having diameters of 0.07–0.25 mm. Section 3 contains pumiceous pebbles and graded beds of granule, sand and clay, with pockets of ash in the lower part. Small nodules and spots of manganese were observed throughout Sections 1 and 2 (Fig. 2). Sedimentary structures indicate that bedding planes are mostly horizontal through all the cores.

Deformation structures

Several types of the deformation structures were recognized on the radiographs (Fujioka *et al.* 1986). They are layer-parallel shear planes, veins, spaced foliations, an asymmetric fold, kink bands, reverse faults and normal faults. The sense of shear, for example sinistral or dextral, is treated in a relative sense on the radiograph for definite description.

Layer-parallel shear planes are dominantly developed in all cores (Figs. 2 and 4) and are identified by gouges (0.1–1.5 mm thick) composed of finer clay, which branch in many cases. The gouge is composed of crushed phyllosilicates in contrast with surrounding platy clay minerals. Boundaries between the gouges and surrounding muds are usually sharp. The layer-parallel shear planes displace veins at about 71 cm from the top of the core (Figs. 2 and 4), showing a sinistral shear; the displacement is approximately 4–6 mm. Original sedimentary laminae are easily distinguished from the shear planes by the fact that they are very thin layers of coarse grains of pyroxenes, feldspars, hornblendes and other minerals greater than 0.1 mm in diameter, as observed in the core above 40 cm and at 84 cm (Figs. 5a & b). Boundaries between laminae and muds are gradual in contrast with those of the shear planes.

Vein structures are found throughout the core. They are recognized as opaque seams at a high angle to the layer and layer-parallel shear planes. The boundaries between the veins and surrounding mud are gradual in contrast to those of layer-parallel shear planes. The

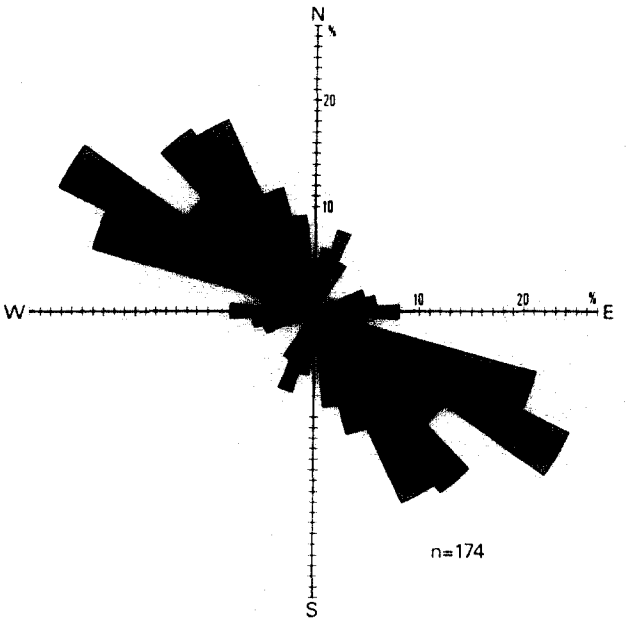

Fig. 3. Rose diagram showing the trends of vein structures, spaced foliations, and reverse faults based on computed tomographic scan images.

veins are filled by phyllosilicates, finer than the surrounding muds. They are not formed by recrystallization, but probably by rearrangement of the *in situ* clay minerals. In intervals at 26 and 30 cm, and between 52 and 57 cm, sigmoidal veins are developed (Figs. 2, 4 and 5a). The bottom of the vein swarms are consistently parallel to layering. The veins are 0.25–0.65 mm in thickness, and were spaced from 1.5 to 6.0 mm apart (Fig. 6a). They have a thick central part which thins towards the margin (Fig. 4). Veins trend approximately NW–SE based on a computed tomography (CT) scan (Figs. 2 and 3). A CT-scan (b in Fig. 2) shows an anastomosing network in the lower part of the sigmoidal veins. The pattern of sigmoidal veins is consistent with sinistral displacement on the layer-parallel shears. The angles between tips of the sigmoidal veins and layer-parallel shear planes range from 37 to 56° and those between the central part of the sigmoidal veins and layer-parallel shear planes range from 71 to 118°. The sigmoidal pattern suggests that they were formed as tension gashes in association with layer-parallel shear. Assuming rotation of the vein centres by simple shear, their sigmoidal shape indicates shear strains of 0.93–1.54 (Fig. 8). The veins cut by layer-parallel shear planes were observed in the core 71 cm from the top. Most of the veins were formed before layer-parallel shear occurred, but anastomosing veins cutting the layer-parallel shear planes and kink bands were found 105 cm from the top of the core (Figs. 5c and 7).

Spaced foliations at high angles to layering are recognized at intervals of depths of 57–58 cm, 62–63 cm, 82–85 cm and 194–195 cm (Fig. 2). The foliations on the radiographs are recognized as opaque seams which only developed in fine layers surrounded by coarser layers. For example, those at 82–85 cm depth are developed in clays in alternating layers of sand and clay (Fig. 5b), and

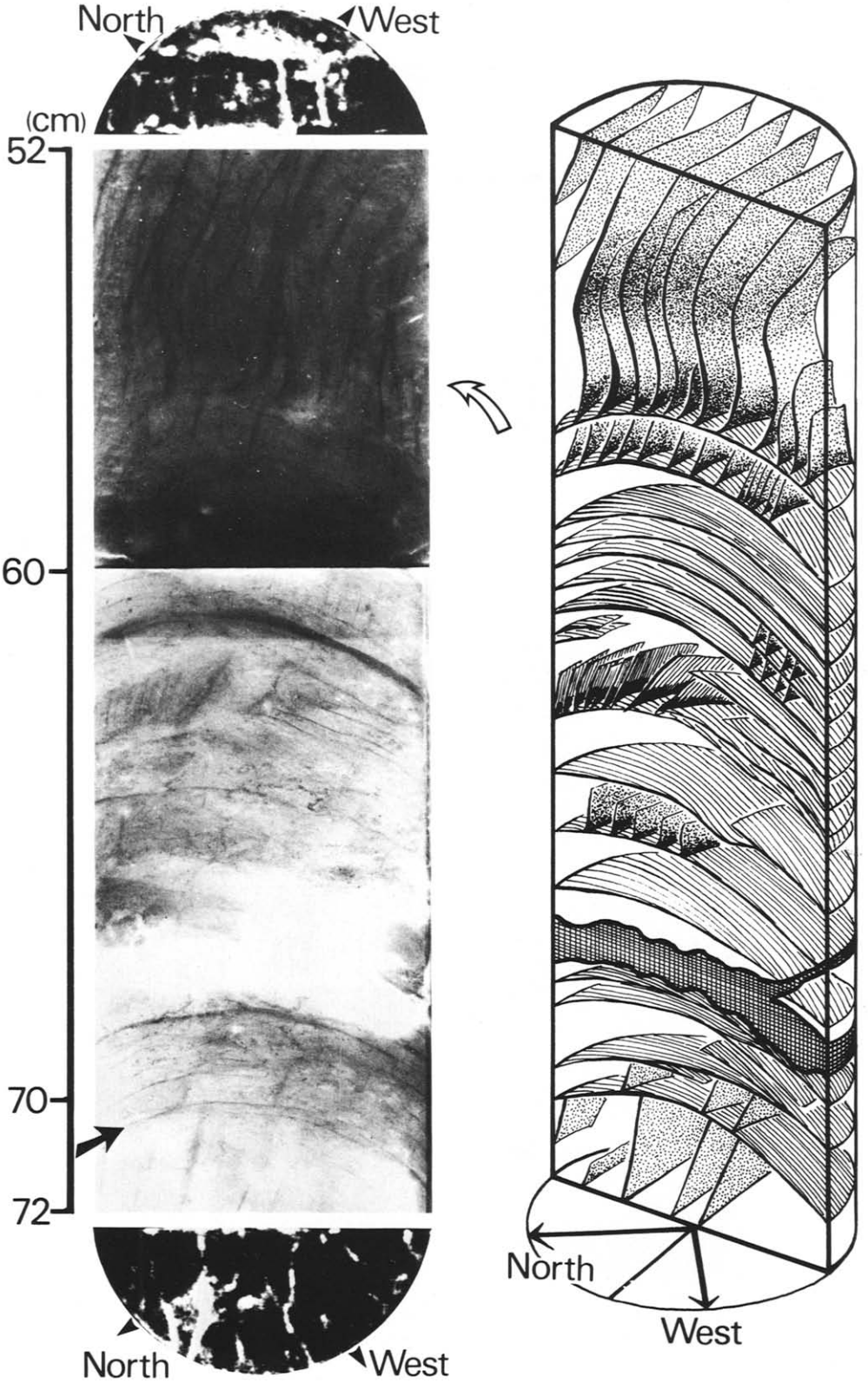

Fig. 4. Radiograph of soft X-ray with computed tomographic scanning (CT-scan) images and three-dimensional reconstruction. The radiograph shows the interval between 52 and 72 cm core depth and the CT-scan images are at 52.5 and 73.5 cm depth in the core. Black and white arrows indicate layer-parallel shear plane and sigmoidal veins, respectively.

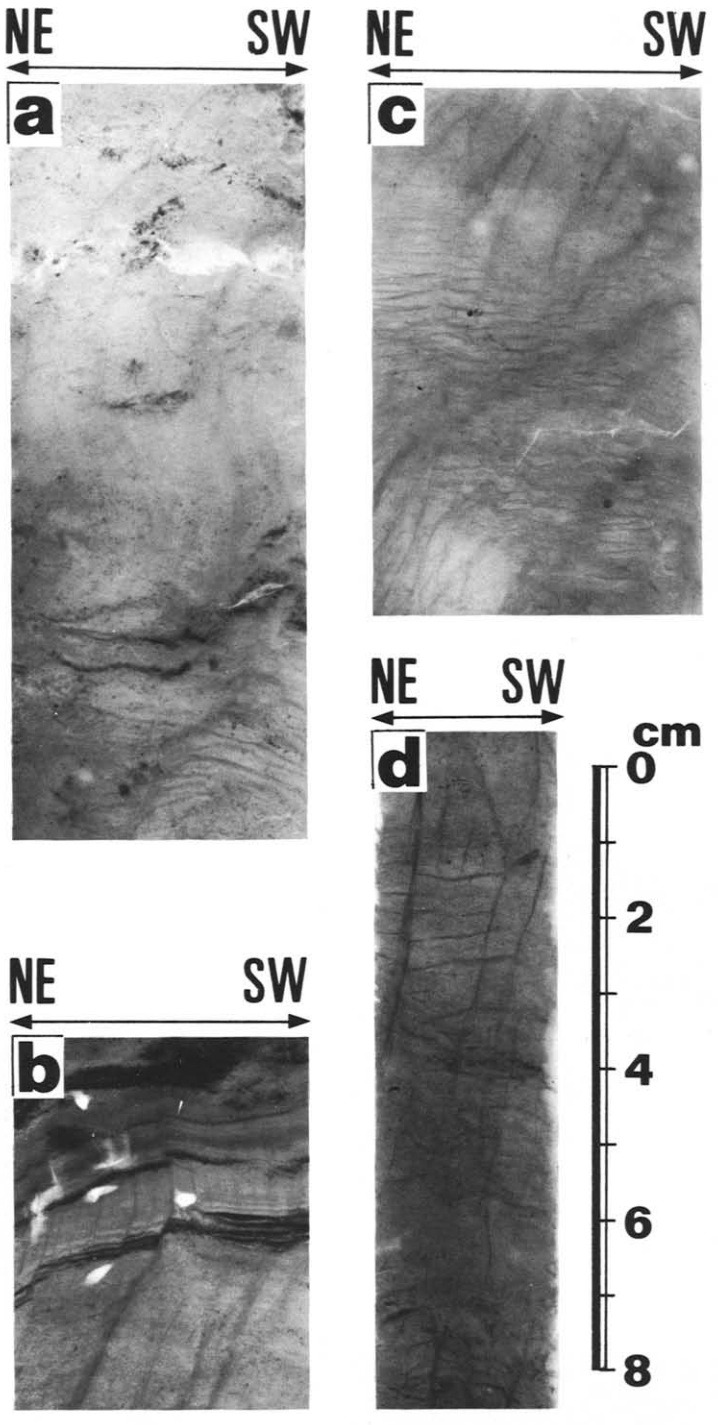

Fig. 5. Deformation structures observed in soft X-ray radiographs. (a) Sigmoidal veins observed in the core interval 23–31 cm. (b) Spaced foliations recognized in clay layer surrounded by coarser layers of black sands at about 83 cm depth. (c) Kink bands developed in the core between 103 and 110 cm; a more detailed sketch is shown in Fig. 7. (d) Reverse faults found from 182 to 190 cm core depth.

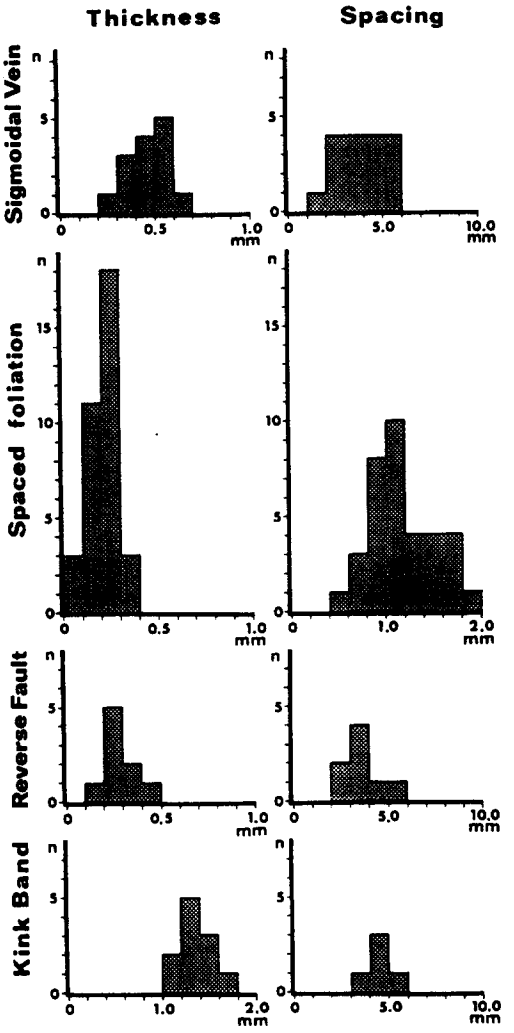

Fig. 6. Histograms showing thickness and spacing of the sigmoidal vein, spaced foliation, reverse fault and kink band. Ordinate *n* represent their observed number.

are composed of fine phyllosilicates arranged parallel to the foliation. The thickness of the foliations are 0.1–0.4 mm, and spaces between foliations range from 0.55 to 1.90 mm (Fig. 6). The foliations trend NW–SE and dip angles relative to layers are from 54 to 90° (Fig. 5b). Their composition is very similar to that of the veins, but they are more closely spaced. Most of the veins have a sigmoidal shape, whereas the foliations show a straight feature. The vein structure develops pervasively in the core, whereas the foliation is observed only in limited layers, especially where fine layers are surrounded by coarser ones.

Reverse faults are found in several parts of the core. They cut laminae at 31 cm core depth and earlier layer-parallel shear planes between 184 and 186 cm (Fig. 5d). Displacements along the faults are from 1 mm to several millimeters. They appear as opaque seams (<0.5 mm) on the radiograph, with sharp boundaries to the surrounding mud (Fig. 6). These boundaries are similar to those of the layer-parallel shear planes but different to those of veins. At 105 cm depth, kink bands change gradually into reverse faults. The dip of the reverse faults range from 62 to 87° and they trend NW at a depth

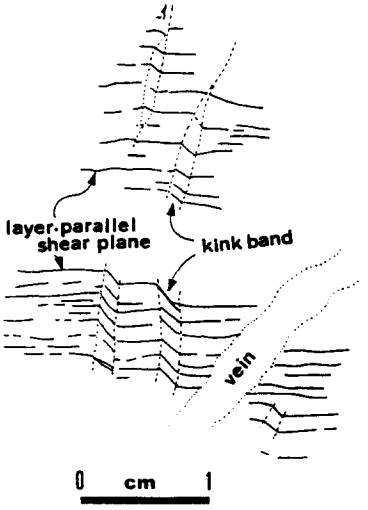

Fig. 7. Expanded sketch of kink bands in Fig. 5(c); note upper lenticular kink band passing into a reverse fault and veins cutting the kink bands and layer-parallel shear planes.

of 182 cm in the core (Fig. 2). Angles between the reverse faults and layer-parallel shear planes range from 65 to 86°.

An asymmetrical fold in a sand layer was found at 82 cm core depth (Fig. 2), with sand flowing into the axial part of the fold and thinning out towards the limb; its similar style indicates that it formed in association with the layer-parallel shearing. The fold shows sinistral shear on the soft X-ray radiograph.

Kink bands were observed at intervals from a depth of 95 to 108 cm in the core. The layer-parallel shear planes are kinked (Figs. 5c and 7). Some bands are lens shaped and their boundaries sometimes pass into reverse faults (Fig. 7). The width of reverse faults continued from the bands are 1.10–1.75 mm (Fig. 6). On the basis of CT scan analysis and profiles of radiographs, the kink band boundaries are sharp and mostly dip southwestward. The kink bands are monoclinic and produce a clockwise

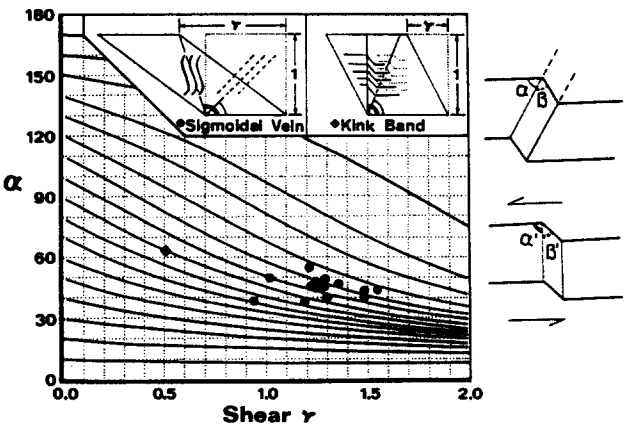

Fig. 8. Shear strains deduced from the sigmoidal veins and the kink bands (graphical solution after Ramsay 1967). Shear strains from the sigmoidal veins are estimated on the basis of anglular relationship between the central part of vein and its tip. In the case of kink bands, it is hypothesized that the angle between the layer-parallel shear planes and kink planes was about 60° before the rotation on the basis of cluster of data in Fig. 9.

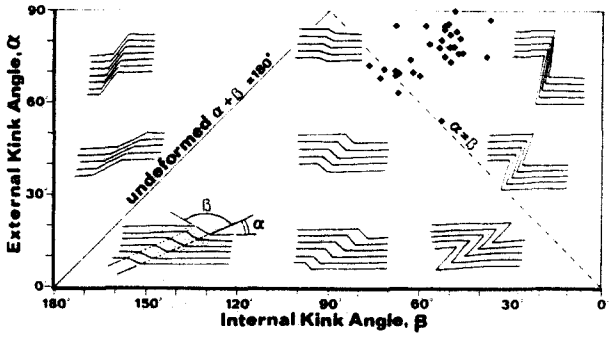

Fig. 9. Relationship between external and internal kink angles (Suppe 1985). Most of the data plot away from the constant volume line ($\alpha = \beta$) with $\alpha > \beta$.

rotation of the layer-parallel shear planes on the radiograph. The stress field deduced from the sense of rotation shows a NE-trending maximum principal axis of compression, oblique to the layering. This stress field is consistent with that estimated from the 'sinistral' layer-parallel shearing. The bands are 1.00–3.00 mm in width. External (α) and internal kink (β) angles range from about 60 to 90° and 80 to 40°, respectively (Fig. 9). The internal kink angle increases with decreasing external angle (Fig. 9) and most of the data plot away from the constant volume line where $\alpha = \beta$. This geometry is unusual and differs from most natural and experimental kink bands (Paterson & Weiss 1962, 1966, Anderson 1964).

Deformation chronology and trend

The deformation stages and trends of the structures cited above are summarized as follows (Fig. 10). The NW-trending vein structures and spaced foliations were formed first and are cut by the layer-parallel shear planes. The layer-parallel shear planes are cut by the NW-trending reverse faults and folded by kink bands. The reverse faults and kink bands appear to have occurred simultaneously, since they pass into each other. All the structures are cut by the youngest vein structures which trend NW–SE. The timing of the asymmetric fold is obscured.

Core induced normal faults are final stage products and are situated at the core margins. Their sense of dislocation is consistent with 'shearing' between the core barrel and core. Whilst the normal faults were induced during core operation, the other structures were not because (1) they are sharply truncated at the core margin and (2) they have no apparent geometrical relations to the core barrel axis or to radial drilling stress.

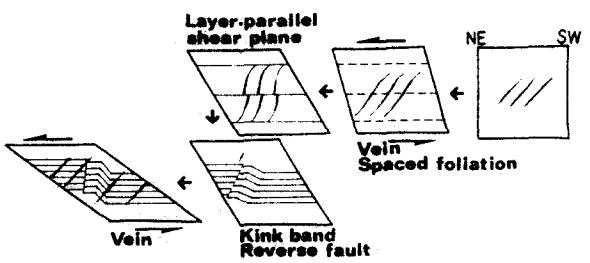

Fig. 10. Progressive shear model for deformation structures in the P-1 core. Volumetric decrease appears to be associated with the deformation in soft sediments.

DISCUSSION AND INTERPRETATION

Difference from other deformed DSDP cores

Three features of this core differ from other DSDP cores.

(1) Tensional structures occur together with compressional ones, features not generally observed together in DSDP cores (Lundberg & Moore 1986).

(2) The deformation features formed at very shallow depth below the sea bed, since the core was recovered from near the sea bottom surface, whereas deformation structures found during DSDP are generally deeper than 100 m below the surface.

(3) Deformation occurs in unlithified soft sediments with a high percentage of pore water, whereas structures in other deformed DSDP cores are from consolidated or semiconsolidated sediments.

Most of the sampling sites of DSDP, with the exception of Nankai Trough and Barbados, are under tensional regimes due to downslope movement, whereas site P-1 is at a compressional convergent plate boundary. This difference in tectonic regime may account for the absence of shallow soft sediment deformation in other DSDP cores. The second possibility for the apparent difference is a difficulty of observation, since we could only detect deformation structures using soft X-ray radiograph. Thirdly, the percentage recovery of shallow soft sediments is very low in the case of the above DSDP sites. The presence of shallow deformation structures is very likely in the lower trench landward slope where the accretionary trench-fill sediments are affected by rapid imposition of tectonic stress or gravity sliding related to tectonism.

Origin of vein structures

Vein structures are known from other DSDP cores and several models of their origin have been proposed. Carson *et al.* (1982) proposed a 'hydrofracturing' model, due to abnormal overpressure caused by tectonic loading in the accretionary wedge. In the case of offshore Guatemala, Dengo (1983) emphasized 'overpressuring' due to decomposition of gas hydrate instead of tectonic loading by accreted sediments. Alternatively, Cowan (1983) suggested that vein structures originate as tension gashes related to simple shear, triggered by slow downslope creep or shearing near fault zones. Ogawa & Miyata (1985) suggested a two stage origin of vein structures at the same localities as Cowan's observation. Early formed veins resulted from overpressuring due to loading by rapid sedimentation and were followed by downslope drag in association with large-scale folding

related to faulting or draping of the slope area (Ogawa & Miyata 1985). Ritger (1985) proposed a model combining hydrofracturing and extension fracturing models. Helm & Vollbrecht (1985) emphasized the high-angle relationship between the veins and layering, suggesting an origin of veins, not as tension gashes but as antithetic Riedel shears, associated with simple shear occurring in anisotropic sediments. Recently Knipe (1986) pointed out that high fluid pressure is not necessary to cause initial failure of veins, and fluid expulsion appears to have been a slow process.

The veins in this study are interpreted as tension gashes associated with shear, as suggested by Cowan (1983) and Knipe (1986). The reasons are as follows: (1) they differ from other shear planes, such as reverse faults and layer-parallel shear planes, which have a very clear gouge zone; (2) their systematic orientation is not consistent with 'hydrofracturing' or 'overpressuring' models which seem to induce a random fabric of veins; (3) their sigmoidal pattern is consistent with the sense of layer-parallel shearing.

The antithetic Riedel shears noted by Helm & Vollbrecht (1985) are not similar to the veins in this study, but may be equivalent to the reverse faults which formed after the layer-parallel shear planes. Helm & Vollbrecht (1985) suggested that antithetic Riedel shears are developed dominantly in association with simple shear imposed on bodies having anisotropic fabrics which are almost parallel to the shear planes.

As the veins are the first deformation structure, there must have been a very high percentage of pore water in the unconsolidated sediments at the time of the formation of the tension gashes. The sigmoidal pattern of the veins gives a quantitative estimate of shear strain along the layering as mentioned before.

Origin of kink bands

Kink bands formed at a later stage and show an unusual relationship between external (α) and internal angles (β), with $\alpha > \beta$. In most natural and experimental kink bands, however, $\alpha \leqq \beta$ (e.g. Paterson & Weiss 1962, 1966, Anderson 1964), since the volume of kink band usually increases or remains constant during kinking.

It seems that there are two possibilities to explain this unusual relationship. The first is that they are formed by homogeneous shear oriented parallel to the kink bands themselves. Anderson (1964) pointed out that this mechanism is an obvious way to make external angles larger than internal angles because layers outside of the kink planes are not connected with those within the kink bands. Dewey (1965) called these "shear kink bands" and suggested a single major shear in the central part of the band. In this study, the observation that kink planes occasionally pass into reverse faults may support such shearing, but most of the kink bands do not show this relationship.

The second possibility is that the kink bands have been modified by later layer-parallel shear. If we start with a typical kink band with $\alpha = \beta = 60°$ and imagine this to have locked in this position, due to its inability to rotate through the bisection angle (Figs. 8 and 10), subsequent deformation by layer-parallel shear will rotate the kink plane and internal foliation. Passive rotation will modify the kink angles to α' and β', such that:

$$\cot (180° - \alpha') = \cot 120° + \gamma$$

$$\cot (180° - \alpha' - \beta') = \cot 60° + \gamma.$$

A final geometry, with $\alpha' = 90°$ and $\beta' = 45°$ can be produced by a shear strain $\gamma = 0.5$ (see Figs. 8 and 10).

We can also consider this layer-parallel shear to have affected veins cutting the kink bands. The veins favoured in the final stage are very similar to those formed in the first stage of deformation, which have been interpreted as tension gashes in association with shear on layer-parallel shear planes. Thus we suggest that the veins cutting the kink bands are also caused by layer-parallel shearing.

A shear strain ($\gamma = 0.50$) estimated from the rotation of the kink band is smaller than $\gamma = 0.93$–1.54 deduced from the rotation of the first formed sigmoidal veins, which may indicate the total shear strain associated with layer-parallel shear (Fig. 8). Consequently, the unusual geometry of kink bands in this study may be related mainly to later deformation caused by subsequent layer-parallel shear. Kink bands in DSDP cores have also been reported from the Nankai Trough (Leg 66) under a compressional regime (Lundberg & Moore 1986), however, there is no detailed geometric analysis of them.

Progressive shear model

A progressive shear and the unconsolidated state of sediments may be appropriate to explain the relationship among the deformation structures. The layer-parallel shear planes appear to be parallel to the principal displacement of the shear. Early deformation produced veins and spaced foliations, which are interpreted as tension gashes associated with layer-parallel shear. The sigmoidal pattern of veins shows the relationship between the gashes and shear (Fig. 8). The reason why the tensional structures were initially dominant may be due to high pore fluid pressure within the unconsolidated sediments. Pore fluid pressure may have risen, due to tectonism or abrupt loading, promoting the development of tension gashes, which were most effective to reduce pore fluid pressure. Deformation at this stage was characterized by particulate flow and rearrangement of the grains, and may have been accompanied by volume decrease in terms of pore reduction and dewatering. Secondary, layer-parallel shear planes are observed pervasively in the core, whereas the displacements along the planes are very small. Moore *et al.* (1986) pointed out that scaly cleavage, which is a slip surface with a small displacement is developed pervasively only in the soft sediments. Since the shear gouges in the soft sediments become harder than surrounding materials after a little slip caused by pore reduction and fluid expulsion, they

are abandoned and new slip surfaces formed, producing pervasive scaly fabric, are developed. The layer-parallel shear planes in this study appear to be similar to scaly foliations observed generally in mudstone from present and ancient accretionary complexes. The timing of folding is uncertain, but it seems early since particulate flow is very clear within the fold. The asymmetric shape of the fold is consistent with the layer-parallel shear.

Reverse faults and kink bands formed at a later stage and the stress fields deduced from their geometry coincide with those estimated from deformation structures in the early stage. This fact suggests that the later deformation also occurred due to subsequent layer-parallel shear. Material conditions, however, seem to have been different from that in the earlier stage, with brittle deformation dominant, since breakage of grains is clear in the shear gouge. The reverse faults and counterclockwise rotation of kink bands are considered as antithetic Riedel shears which are developed in anisotropic materials having fabric parallel to principal displacement (Helm & Vollbrecht 1985). Unusual kink bands whose external angles are larger than internal ones, and veins developed in the latter suggest that layer-parallel shear was still going on, since this sediment is not yet consolidated.

In conclusion, the deformation observed in the core P-1 progressed in association with volume decrease due to pore reduction and fluid expulsion during the consolidating process. This pattern is very different from the rather simple pattern of deformation reported from other DSDP cores and may depend on differences of tectonic setting. The site P-1 is at a very complicated situation in the Mariana–Yap junction area. The NNW-trending vein structures and shear planes are almost parallel to the trend of the northeastern slope of the unnamed swell shown in Fig. 1. This fact suggests either rapid northeastward down-slope creep or incipient subduction along the eastern foot of the unnamed swell. The second possibility is suspected since the lack of volcanic activity in Yap Island seems to be related to the accretion and buoyant subduction of the unnamed swell and the Caroline Ridge.

Acknowledgments—We thank all the scientific and crew members of the R/V Hakuho Maru, Ocean Research Institute, University of Tokyo, for the cruise of KH86-1, especially, Professor Y. Tomoda, chief scientist of the cruise, who has continuously encouraged us during the preparation of the manuscript. Y. Ogawa and A. Takeuchi read the manuscript critically and discussions about magnetization with T. Furuta are gratefully acknowledged. We are also grateful to M. Okamura and H. Matsugi for their paleontological determination of the core. We express sincere thanks to W. Sou, A. Taira and K. Kosaka for their valuable suggestions of this problem. D. J. Sanderson and two anonymous reviewers gave us very useful suggestions, which we also appreciate very much. This work was supported partly by funds from the Co-operative Program (No. 86131 and No. 86175) provided by the Ocean Research Institute, University of Tokyo, in 1986.

REFERENCES

Anderson, T. B. 1964. Kink bands and related geological structures. *Nature* **202**, 272–274.

Bukry, D., Douglas, R. G., Kling, S. A. & Krasheninnikov, V. 1971. Planktonic microfossil biostratigraphy of the northwestern Pacific Ocean. *Init. Reps DSDP* **6**, 1253–1300.

Carson, B., Von Huene, R. & Arthur, M. 1982. Small-scale deformation structures and physical properties related to convergence in Japan trench slope sediments. *Tectonics* **1**, 277–302.

Cowan, D. S. 1983. Origin of "Vein Structure" in slope sediments on the inner slope of the Middle America Trench off Guatemala. *Init. Reps DSDP* **67**, 645–650.

Dengo, C. A. 1983. A structural analysis of cores from the leg 67 transect across the Middle America Trench-Offshore Guatemala. *Init. Reps DSDP* **67**, 651–666.

Dewey, J. F. 1965. Nature and origin of kink bands. *Tectonophysics* **1**, 459–494.

Fujioka, K., Furuta, T., Kimura, G., Kodama, K., Koga, K., Kuramoto, S., Matsugi, H., Seno, T., Takeuchi, A., Watanabe, M. & Yamamoto, S. 1986. Sediments and rocks in and around the Palau and Yap Trenches. *Reps Hakuho Maru Cruise KG86-1, Ocean Res. Inst. Univ. Tokyo.* 38-148.

Helm, R. & Vollbrecht, A. 1985. Brittle–ductile shear zones in slope sediments off Guatemala, sites 568 and 569. Deep Sea Drilling Project Leg 84. *Init. Reps DSDP* **84**, 625–632.

Knipe, R. J. 1986. Microstructural evolution of vein arrays preserved in Deep Sea Drilling cores from the Japan Trench, Leg 57. *Mem. geol. Soc. Am.* **166**, 75–87.

Lundberg, N. & Moore, J. C. 1986. Macroscopic structural features in Deep Sea Drilling Project cores from forearc regions. *Mem. geol. Soc. Am.* **166**, 13–44.

Minster, J. B. & Jordan, T. H. 1979. Present day plate motions. *J. geophys. Res.* **83**, 5331–5345.

Moore, J. C., Roeske, S., Lundberg, N., Schoonmaker, J., Cowan, D. S., Gonzales, E. & Lucas, S. E. 1986. Scaly fabrics from Deep Sea Drilling Project cores from forearcs. *Mem. geol. Soc. Am.* **166**, 55–73.

Ogawa, Y. & Miyata, Y. 1985. Vein structure and its deformation history in the sedimentary rocks of the Middle America Trench slope off Guatemala, Deep Sea Drilling Project Leg 84. *Init. Reps DSDP* **84**, 811–829.

Paterson, M. S. & Weiss, L. E. 1962. Experimental folding in rocks. *Nature* **195**, 1046–1048.

Paterson, M. S. & Weiss, L. E. 1966. Experimental deformation and folding in phyllite. *Bull. geol. Soc. Am.* **77**, 343–347.

Ramsay, J. G. 1967. *Folding and Fracturing of Rocks.* McGraw-Hill, New York.

Ritger, S. D. 1985. Origin of vein structures in the slope deposits of modern accretionary prisms. *Geology.* **33**, 437–439.

Suppe, J. 1985. *Principles of Structural Geology.* Prentice-Hall, Englewood Cliffs, New Jersey, 336–340.